

Designing Balanced Surfactants for Mixtures of Immiscible Polymers

J. H. Lee,[†] N. P. Balsara,^{*,†} R. Krishnamoorti,^{*,‡}
H. S. Jeon,[§] and B. Hammouda[⊥]

Department of Chemical Engineering, University of California, Berkeley, California 94720; Department of Chemical Engineering, University of Houston, Houston, Texas 77204; Department of Petroleum and Chemical Engineering, New Mexico Tech, 801 Leroy Place Socorro, New Mexico 87801; and National Institute of Standards and Technology, Building 235, E 151, Gaithersburg, Maryland 20899

Received June 18, 2001

Microemulsions, wherein comparable amounts of immiscible substances like oil and water are interspersed by the addition of carefully chosen surfactants, are of considerable interest.^{1–3} The formation of these phases requires flexible interfaces between the oil- and water-rich domains, which, in turn, require a balance between the hydrophilic and hydrophobic characteristics of the surfactant. The phase diagram obtained along the isopleth when a balanced surfactant is added to a 50/50 mixture of oil and water has the shape of a fish,¹ as shown schematically in Figure 1. Most of the literature on balanced surfactants is restricted to aqueous systems. In a few examples, water has been replaced by other polar molecules such as formamide and glycol.^{4,5} In all of these systems polarity and hydrogen bonding are believed to play an important role in establishing the required balance. To our knowledge, the principles for designing balanced surfactants for immiscible non-polar substances have not been established. The purpose of this paper is to address this shortcoming.

A striking feature of the oil/water/balanced surfactant (O/W/BS) phase diagram is the presence of several reentrant phase transitions, as shown in Figure 1. Two-phase (2P) regions appear at low and high temperatures outside the fish. Microemulsions (M), which are formed in the tail of the fish, are flanked by a three-phase (3P) window at low surfactant concentration and an ordered lamellar phase (L) at high surfactant concentration.

Pioneering work by Bates, Lodge, and co-workers^{6–8} demonstrated that the addition of an A–B diblock copolymer can result in the formation of microemulsions in mixtures of (nonpolar) A and B homopolymers. The phase behavior of A/B/A–B mixtures is quite different from that shown in Figure 1. There are no reentrant phase transitions in these systems, and the microemulsion phase is restricted to a narrow channel between the two-phase and lamellar phases. In addition, for a given chemical system, the microemulsion phase is obtained over a limited range of homopolymer molecular weights ($N \approx 2/\chi$ where N is the number of repeat units per homopolymer chain, and χ is the Flory–Huggins interaction parameter for A/B interactions).

In this paper we demonstrate that a polyethylene-block-head-to-head polypropylene copolymer (PE–PP) exhibits many of the properties of a balanced surfactant in mixtures of polyisobutylene (PIB) and polyethylene

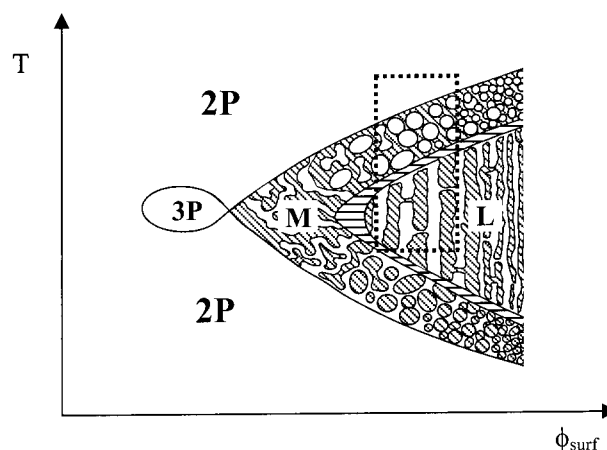


Figure 1. Typical phase diagram for oil/water/balanced surfactant (temperature vs surfactant volume fraction). M = microemulsion, L = lamellae, 2P = 2 phases, 3P = 3 phases. The hatched region between the L and M phases is the region where both L and M phases coexist. The dashed rectangle indicates the limits of our experimental window ($113\text{ °C} \leq T \leq 210\text{ °C}$ and $0.15 < \phi_{\text{surf}} \leq 0.30$).

(PE). We arrived at our choice of materials by examining the intermolecular interactions in O/W/BS mixtures¹ and duplicating them in the polymeric system. In particular, we build on the efficacy of alkyl polyglycol ethers (often referred to as nonionic surfactants) for producing oil/water microemulsions.¹ Oil and water are grossly incompatible with each other. This is not difficult to duplicate in polymeric systems because most polymers are immiscible in each other, and PE and PIB are no exceptions.⁹ Surfactant/oil interactions are generally simple, and homogeneous solutions are obtained above the upper critical solution temperature (UCST). Similarly, the interactions between PE and PP homopolymers are simple and lead to a UCST.^{10,11} PE is thus our analogue of oil. The key to the formation of the fish phase diagram is the nature of surfactant/water interactions. The solubility of ethylene oxide chains in water decreases with increasing temperature, leading to a lower critical solution temperature (LCST).¹ Mixtures of PIB and PP homopolymers also exhibit an LCST.¹² Thus, we chose PIB to mimic water and PE–PP to mimic the nonionic surfactant. We have thus designed a polymeric system, based entirely on hydrocarbon molecules without specific interactions or permanent dipoles, that is capable of exhibiting all of the characteristics of a balanced surfactant system.

The chemical simplicity of the components (empirical formula is CH_2 in all cases) allows us to characterize the intermolecular interactions by the Flory–Huggins parameters χ_{ij} (where $i, j = \text{PE}, \text{PP}, \text{or PIB}$). The χ parameters between PE/PP ($\chi_{\text{PE/PP}}$) and PIB/PP ($\chi_{\text{PIB/PP}}$) have been measured by small angle neutron scattering (SANS).^{10,12} The usual temperature dependence $\chi = A + B/T$ is observed in both blends: $\chi_{\text{PE/PP}} = -0.018 + 11.0/T$ and $\chi_{\text{PIB/PP}} = 0.018 - 7.7/T$ (reference volume = 100 Å^3). We chose the PE/PIB/PE–PP system because the parameter B for PE/PP and PIB/PP blends have similar magnitude but opposite sign. We thought that this might be the key for balancing the PIB-philic and PIB-phobic tendencies of the PE–PP surfactant. In addition, following the nonionic surfactant literature,¹

[†] University of California.

[‡] University of Houston.

[§] New Mexico Tech.

[⊥] National Institute of Standards and Technology.

we chose a PE–PP block copolymer that was weakly ordered in the bulk. The order–disorder transition temperature of the bulk PE–PP sample was determined to be 149 ± 2 °C.¹⁰

The PE and PE–PP samples were synthesized by anionic polymerization of dienes followed by saturation of the double bonds with deuterium.¹⁰ The PIB sample was synthesized by cationic polymerization.¹³ The weight-averaged molecular weights of the components M_i were determined by methods described in ref 10 and found to be $M_{PE} = 12$ kg/mol, $M_{PIB} = 14$ kg/mol, $M_{PE-PP} = 66$ kg/mol, volume fraction of PE in PE–PP is 0.49. All the components are amorphous liquids in the temperature range of the experiments ($113 \leq T \leq 210$ °C). In the mean-field limit, the thermodynamic interactions between polymer chains are controlled by the product of χ and M_i . M_{PE} was thus chosen to be slightly smaller than M_{PIB} , because the magnitude of parameter B of the PE/PP system is slightly larger than that of the PIB/PP system.¹⁴ The average hydrogen to deuterium atom ratio in the PE chains is 2.2, and those in the PE and PP chains of the block copolymer are 1.0 and 2.4, respectively. The unperturbed radii of gyration of the molecules, $R_{g,i}$, were estimated from the statistical segment length data: $R_{g,PIB} = 4.1$ nm, $R_{g,PE} = 5.2$ nm, and $R_{g,PE-PP} = 12.7$ nm. Blends with equal weights of PE and PIB with varying amounts of PE–PP were prepared. SANS experiments, from samples labeled B15, B20, and B30 that contained 15, 20, and 30 vol % block copolymer, respectively, were conducted on the NG3 beamline at the National Institute of Standards and Technology (NIST) in Gaithersburg, MD. The dashed rectangle in Figure 1 represents the experimental window covered by the current experiments (details given below). We report the azimuthally averaged scattering intensity, I , as a function of q [$q = 4\pi \sin(\theta/2)/\lambda$, θ is the scattering angle and λ , the wavelength of the incident neutrons, was 1.2 nm].^{10,11}

Binary PE/PIB blends were extremely turbid with a milklike appearance in our temperature window, indicating that χ is significantly larger than $2/N$ for these blends ($N \approx 250$ based on a reference volume of 100 \AA^3). The addition of the PE–PP block copolymer led to a significant reduction in turbidity. Sample B15 was translucent, while sample B20 and samples with larger surfactant concentrations were clear.

Since our main interest is in microemulsions and lamellar phases, and both these phases in O/W/BS systems are optically clear, we begin by studying the SANS intensity vs q from B20 at selected temperatures; see Figure 2a. At temperatures below 145 °C, we see a primary scattering peak at $q_1 = 0.07 \text{ nm}^{-1}$ and a second-order peak at $q_2 = 0.14 \text{ nm}^{-1}$, indicating the presence of an ordered lamellar phase ($q_2 = 2q_1$) with a characteristic length $d = 2\pi/q_1 = 90$ nm. The peaks at q_1 and q_2 are superposed on a monotonically decaying function of q (see Figure 2a). This additional scattering is expected because of correlations arising from the chainlike character of the components that form the lamellar phase^{7,8,10,11} (note that both PE and PE–PP are labeled with deuterium). The I vs q data at low q ($q < 0.04 \text{ nm}^{-1}$) thus exhibit a negative slope (Figure 2a); if the scattering were due to lamellae only, this slope would be positive. The SANS data in the vicinity of the second-order peak were fit to the form of $I = C \exp[-(q - q_{\text{peak}})^2/\sigma^2] + I_{\text{background}}(q)$ where $1/I_{\text{background}}(q)$ is a quadratic function of q , with C , σ , and the quadratic coefficients

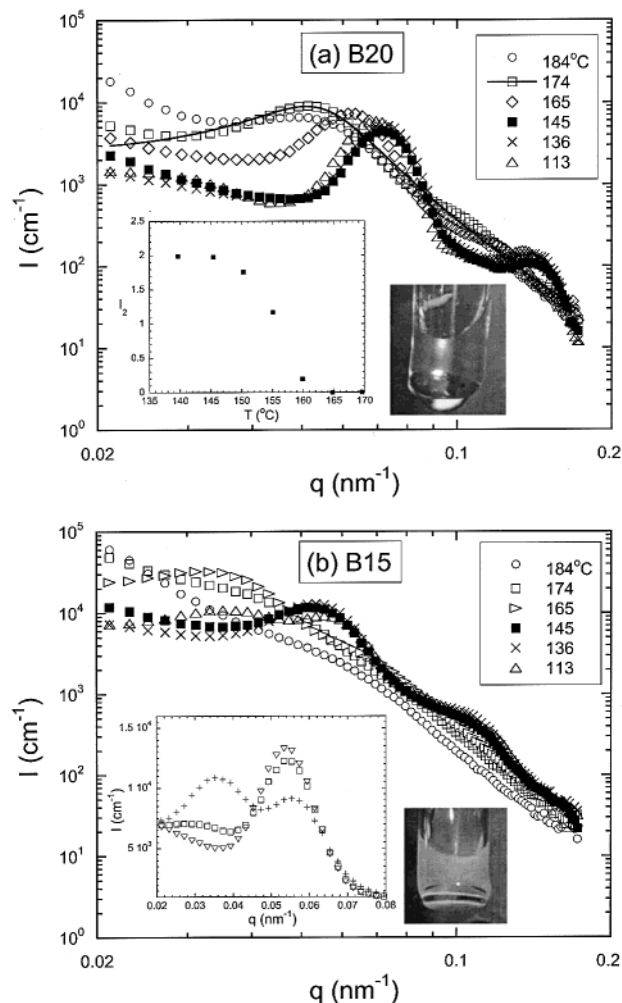


Figure 2. SANS profiles of (a) B20 ($\phi_{\text{surf}} = 0.20$) and (b) B15 ($\phi_{\text{surf}} = 0.15$) at selected temperatures. (a) Inset: temperature dependence of I_2 of B20. (b) Inset: B15 SANS profiles at $T \leq 120$ °C: +, 113 °C; □, 116 °C; ▽, 120 °C. The curve in (a) represents the least-squares Teubner–Strey fit through data ($a = 4.35 \times 10^{-4}$, $b = -0.25$, $c = 48.14$) obtained in the microemulsion phase at $T = 174$ °C. Photographs of both samples in a vacuum oven at 136 °C are also shown.

as adjustable parameters. In the inset in Figure 2a we plot the area under the second-order peak I_2 ($I_2 = \sqrt{\pi C \sigma}$) as a function of temperature. I_2 is zero above 160 °C, indicating the absence of lamellae at temperatures above 160 °C.

The primary peak of sample B20, however, persists at temperatures between 165 and 180 °C (Figure 2a). The SANS data in this temperature window are consistent with the Teubner–Strey (T–S) model [$I(q) = 1/(a + bq^2 + cq^4)$] for scattering from microemulsions (I_2 is zero in this temperature range).^{1–8,11} Typical agreement between the T–S model and our data is shown in Figure 2a; the curve represents a least-squares T–S fit through the 174 °C data.¹⁵ The agreement between the T–S model and the data indicates the presence of a microemulsion phase at temperatures between 165 and 180 °C. At temperatures ≥ 184 °C, there is a large increase in the SANS intensity at low q ($q < 0.03 \text{ nm}^{-1}$), indicating macrophase separation above 184 °C. Light scattering experiments indicated that the cloud point of B20 is located at 180 ± 5 °C, confirming the macrophase separation transition inferred from SANS. (The light scattering data are unremarkable and hence not shown.)

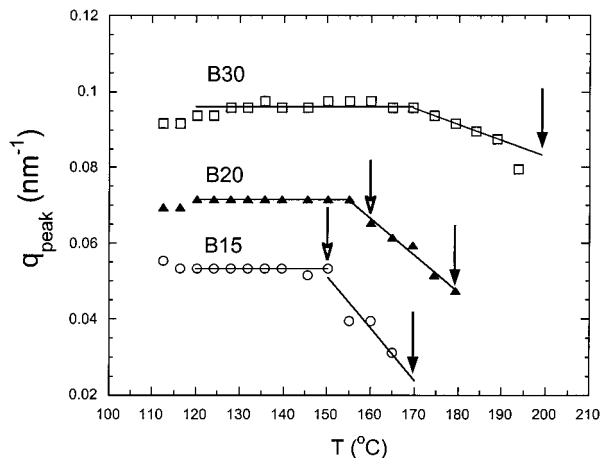


Figure 3. Temperature dependence of the primary peak position q_1 of samples B15 ($\phi_{\text{surf}} = 0.15$), B20 ($\phi_{\text{surf}} = 0.20$), and B30 ($\phi_{\text{surf}} = 0.30$). The lamellar to microemulsion and microemulsion to two-phase transitions are identified by open and filled arrowheads, respectively.

In Figure 2b we show SANS data obtained from sample B15. The scattering profile at $T = 136$ °C is similar to that obtained from B20: a primary peak at $q_1 = 0.05$ nm⁻¹ and a second-order peak at $q_2 \approx 2q_1$. This indicates a lamellar structure with a period of 130 nm. Note, however, that this sample is translucent at 136 °C (see photographs in Figure 2). This is quite different from O/W/BS and polymeric A/B/A–B systems, wherein both microemulsion and lamellar phases are optically clear. The lack of transparency of B15 is probably due to the fact that the characteristic length scale of the lamellar structure is comparable to the wavelength of light. Additional contributions to the scattered light may arise due to the undulations of such highly swollen lamellae ($d \gg R_{g,i}$). The data in Figure 2a,b indicate that the phase behaviors of B15 and B20 are qualitatively similar. On the basis of the criteria used to interpret the SANS data from B20, we conclude that for B15 the lamellar to microemulsion and microemulsion to two-phase transitions occur at 150 ± 5 and 170 ± 5 °C, respectively.

In Figure 3 we show the temperature dependence of the primary peak position q_1 for samples B15, B20, and B30. In all cases we see a range of temperatures where the peak position is independent of temperature (indicated by a horizontal line in Figure 3). At high temperatures we see a decrease in q_1 in all three samples. The arrows with unfilled heads indicate the temperature above which I_2 vanished, signifying the lamellar to microemulsion transition.¹⁶ In both B15 and B20, the disappearance of the second-order peak and the decrease of q_1 occurs at the same temperature (within experimental uncertainty). The onset of the decrease in q_1 thus appears to be a signature of the lamellar to microemulsion transition. It is evident in Figure 3 that the characteristic length of the microemulsions is larger than that of the lamellae for a given PE–PP concentration. In addition, temperature has a larger effect on the characteristic length of the microemulsions than that of the lamellae. The arrows with the filled heads in Figure 3 indicate the microemulsion to two-phase transition. It is evident that both lamellar to microemulsion and microemulsion to two-phase transitions occur at higher temperatures as the surfactant concentration is increased. This is entirely consistent with the

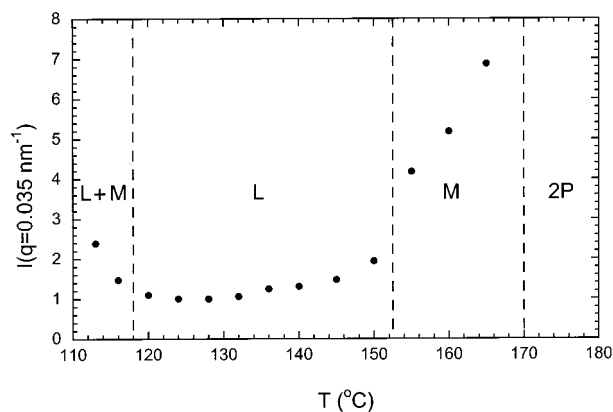


Figure 4. Temperature dependence of SANS intensity at $q = 0.035$ nm⁻¹ of sample B15 ($\phi_{\text{surf}} = 0.15$) with identification of lamellar (L), microemulsion (M), and two-phase (2P) windows. The window of coexistence of L and M at high temperature, as required by the Gibbs phase rule, was not identified possibly due to the coarseness of our temperature steps.

fish phase diagram shown in Figure 1 (see dashed rectangle).

Sample B15 shows clear evidence of a reentrant phase transition. In the inset in Figure 2b we show the SANS data obtained at temperatures ≤ 120 °C. An increase in the low- q scattering is observed at $q \approx 0.035$ nm⁻¹. This is made clear in Figure 4 where we plot $I(q = 0.035$ nm⁻¹) vs temperature for B15 along with the identification of the temperature-dependent phases in the sample. The increase in low- q scattering at high temperatures is an announcement of the lamellar to microemulsion transition. We see a similar increase in low- q scattering at low temperatures (≤ 116 °C) in B15 and the emergence of a new scattering peak at $q = 0.035$ nm⁻¹ (see inset of Figure 2b). This peak is qualitatively similar to that obtained from the high-temperature microemulsions. However, the lamellar peaks at $q_1 = 0.055$ nm⁻¹ and $q_2 = 2q_1$ persist down to 113 °C. This indicates the coexistence of lamellae and microemulsions. Similar coexistence was obtained by Washburn et al. at the lamellar/microemulsion boundary in polymeric A/B/A–B systems⁸ and O/W/BS microemulsions.² Coexistence of lamellar and microemulsion phases is required by the Gibbs phase rule at the lamellar/microemulsion boundary, as indicated in Figure 1. The low-temperature lamellar to microemulsion transition is thus located near the bottom of our experimental window, as shown qualitatively in Figure 1. The increase in low- q scattering upon cooling is not seen in B20 (Figure 3a) and B30 (not shown). On the basis of Figure 1, we expect the low-temperature lamellar to microemulsion transitions in B20 and B30 to occur at temperatures below 113 °C.

In summary, we have shown a new methodology for designing balanced surfactants for mixtures of immiscible polymers, based on the temperature dependence of the Flory–Huggins interaction parameters χ . Mixtures of highly incompatible A/B homopolymers (χ much larger than $2/N$) were organized into microemulsions by the introduction of a suitably designed A–C block copolymer. This is a significant departure from the large body of previous experimental and theoretical work in the field of polymer blends (refs 5–8, 10, 11, 14, 17, 18, and references therein), which relied on the surfactancy of A–B block copolymers for organizing A/B mixtures. Since the temperature dependencies of χ of

many polymer pairs are known,¹⁹ our findings can be generalized to design balanced surfactants for a wide variety of polymer blends. For example, we propose that poly(vinyl methyl ether)-*block*-polybutadiene copolymers are likely to serve as balanced surfactants for polystyrene/polybutadiene blends. Our work demonstrates a pathway for designing balanced surfactants in systems such as hydrocarbon mixtures wherein specific interactions and permanent dipoles are absent.

While we have demonstrated that the PE-PP block copolymer exhibits many of the characteristics found in balanced surfactants, our study is far from complete. It is important to recognize that the identification of fish phase diagrams in O/W/BS systems with accessible reentrant phase diagrams (between 0 and 100 °C) required decades of experimental and theoretical work.¹⁻⁵ We are optimistic that the principles for designing balanced surfactants for immiscible polymers will be rapidly identified, due to valuable insight from previous studies of O/W/BS and A/B/A-B systems,^{1-8,10,11} and the fact that many of the theories for A/B/A-B mixtures^{14,17,18} can easily be adapted for A/B/A-C systems.

Acknowledgment. Financial support, provided by the NSF (CTS-0196066, DMR-9901951, and DMR 9875321), helpful discussions with Eric Kaler, and helpful comments of the referees are gratefully acknowledged. The SANS instrument is supported by Grant DMR-9986442 from the National Science Foundation to NIST.²⁰

References and Notes

- (1) Kahlweit, M.; Strey, R. *Angew. Chem., Int. Ed. Engl.* **1985**, *24*, 654.

- (2) Strey, R. *Colloid Polym. Sci.* **1994**, *272*, 1005.
- (3) Chen, S. H.; Choi, S. M. *Supramol. Sci.* **1998**, *5*, 197.
- (4) Schubert, K. V.; Busse, G.; Strey, R.; Kahlweit, M. *J. Phys. Chem.* **1993**, *97*, 248.
- (5) Martino, A.; Kaler, E. W. *Langmuir* **1995**, *11*, 779.
- (6) Bates, F. S.; Maurer, W.; Lodge, T. P.; Schulz, M. F.; Matsen, M. W.; Almdal, K.; Mortensen, K. *Phys. Rev. Lett.* **1995**, *75*, 4429.
- (7) Hillmyer, M. A.; Maurer, W. W.; Lodge, T. P.; Bates, F. S.; Almdal, K. *J. Phys. Chem. B* **1999**, *103*, 4814.
- (8) Washburn, N. R.; Lodge, T. P.; Bates, F. S. *J. Phys. Chem. B* **2000**, *104*, 6987.
- (9) Flory, P. J.; Eichinger, B. E.; Orwoll, R. A. *Macromolecules* **1968**, *1*, 287.
- (10) Jeon, H. S.; Lee, J. H.; Balsara, N. P. *Macromolecules* **1998**, *31*, 3328.
- (11) Jeon, H. S.; Lee, J. H.; Balsara, N. P.; Newstein, M. C. *Macromolecules* **1998**, *31*, 3340.
- (12) Krishnamoorti, R.; Graessley, W. W.; Fetters, L. J.; Graner, R. T.; Lohse, D. J. *Macromolecules* **1995**, *28*, 1252.
- (13) Storey, R. F.; Chisholm, B. J.; Bryan, B. L. *Macromolecules* **1995**, *28*, 4055.
- (14) This approximation is not valid in the regime where fluctuations are dominant as shown in: Kielhorn, L.; Muthukumar, M. *J. Chem. Phys.* **1997**, *107*, 5588.
- (15) Teubner, M.; Strey, R. *J. Chem. Phys.* **1987**, *87*, 3159. The small deviations between the Teubner-Strey fits and the data (174 °C data in Figure 2a) at low q are probably due to chain contributions to the scattering, while those at high q are similar to those seen in O/W/BS microemulsions and are attributed to the crossover from Teubner-Strey scattering to Porod scattering.³
- (16) The higher-order peak was outside the q -window for B30.
- (17) Broseta, D.; Fredrickson, G. H. *J. Chem. Phys.* **1990**, *93*, 2927.
- (18) Janert, P. K.; Schick, M. *Macromolecules* **1997**, *30*, 3916.
- (19) Balsara, N. P. *Physical Properties of Polymers Handbook*; AIP Press: New York, 1996; Chapter 19.
- (20) NIST does not necessarily endorse the products and chemicals named in this paper.

MA011038E